



Differentiation of human iPSCs into VSMCs and generation of VSMC-derived calcifying vascular cells

Anja Trillhaase^{a,e,f}, Undine Haferkamp^{a,d,e,f}, Alexandra Rangnau^{a,e,f}, Marlon Märtens^{a,e,f},
Beatrice Schmidt^{a,e,f}, Michaela Trilck^b, Philip Seibler^b, Redouane Aherrahrou^{a,c,e,f},
Jeanette Erdmann^{a,e,f,1}, Zouhair Aherrahrou^{a,e,f,*}

^a Institute for Cardiogenetics, University of Luebeck, Germany

^b Institute for Neurogenetics, University of Luebeck, 23562 Luebeck, Germany

^c Center for Public Health Genomics, Department of Biomedical Engineering, University of Virginia, Charlottesville, VA 22908, USA

^d Fraunhofer Institute for Molecular Biology and Applied Ecology (IME), 22525 Hamburg, Germany

^e DZHK (German Centre for Cardiovascular Research), Partner Site Hamburg/Kiel/Luebeck, Germany

^f University Heart Centre Luebeck, 23562 Luebeck, Germany

ABSTRACT

Vascular calcification displays a major cause of death worldwide, which involve mainly vascular smooth muscle cells (VSMCs). Since 2007, there are increasing numbers of protocols to obtain different cell types from human induced-pluripotent stem cells (iPSCs), however a protocol for calcification is missing.

Few protocols exist today for the differentiation of iPSCs towards VSMCs and none are known for their calcification. Here we present a protocol for the calcification of iPSC-derived VSMCs. We successfully differentiated iPSCs into VSMCs based on a modified protocol. Calcification in VSMCs is induced by a commercial StemXVivo™ osteogenic medium. Calcification was verified using Calcein and Alizarin Red S staining or Calcium assays, and molecular analyses showed enhanced expression of calcification-associated genes.

The presented method could help to study genetic risk variants, using the CRISPR/Cas technology through the introduction of Knockouts or Knockins of risk variants. Finally, this method can be applied for drug screening.

1. Introduction

Vascular diseases increase the risk for coronary artery diseases (CAD), which are characterized by atherosclerosis and calcification deposits within the vessels. These pathogenic deposits lead to a narrowing of vessel lumen and subsequent decrease in oxygen supply resulting in myocardial infarction (MI) of the surrounding area, clinically known as heart attack. Hyperlipidaemia, hypertension, diabetes, chronic renal insufficiency, obesity, smoking, and increasing age favour the development of CAD (Torpy et al., 2009; Wilson et al., 1998).

In addition to these traditional risk factors, genetic components also play an important role in the development of CAD. Genetic variants increase the risk of predisposition to CAD (Webb et al., 2017). Our group contributed largely to the identification of 164 genetic loci that are significantly associated with CAD using genome-wide association studies (GWAS) (Samani et al., 2007; Schunkert et al., 2011; CARDIoGRAMplusC4D Consortium, 2013). Among these identified CAD risk loci, five loci show also significant association with coronary artery calcification (CAC) including 9p21, *ADAMTS7*, *PHACTR1*,

MRAS, and *COL4A1/COL4A2* (Webb et al., 2017). Our group reported very recently that *PHACTR1* modulates the severity of calcification in mouse embryonic stem cell-derived SMCs, and its gene expression increases with calcification in human SMCs (Aherrahrou et al., 2017).

Vascular calcification is described as the deposition of CaP mineral, usually as hydroxyapatite or inorganic phosphate (Pi), in cardiovascular tissues, like arteries, heart valves and the cardiac muscle (Jono et al., 2000a). It is associated with the development of atherosclerotic intimal lesions and a common consequence of aging (Jono et al., 2000b). Vascular calcification is associated with a three- to four-fold increase in the risk of cardiovascular morbidity and mortality (Alam et al., 2009). One of the major cell types involved in vascular calcification are vascular smooth muscle cells (VSMCs). Calcifying VSMCs lose their expression of SMC-typical genes like Transgelin (*TAGLN*), Calponin (*CNN1*), or Caldesmon 1 (*CALD1*), and start expressing osteogenic markers, such as *CTSK* and *ALP* (Alam et al., 2009; Doherty et al., 2003; Drake et al., 1996; Lutgens et al., 2007; Thompson and Towler, 2012). Consequently, they deposit bone-like minerals like CaP in the extracellular matrix (ECM) (Alam et al., 2009; Balderman et al.,

* Corresponding author at: Institute for Cardiogenetics, University of Luebeck, Maria-Goeppert-Str. 1, 23562 Luebeck, Germany.

E-mail address: zouhair.aherrahrou@uni-luebeck.de (Z. Aherrahrou).

¹ Denotes equal contribution.

2012; Byon et al., 2008; Tintut et al., 2003), that contributes to the calcification of blood vessels. It is known, that primary VSMCs quickly lose their phenotypic properties *in vitro* that rises various complications for their use in long term experiments *in vitro*, and requires verification of the results *in vivo* (Alexander and Owens, 2012). Further, primary VSMCs lose their proliferative activity with increasing donor age, and puts donors at high risks for the isolation of cells, as a surgical intervention is necessary to access primary VSMCs (Dash et al., 2015). Therefore, iPSC-derived VSMCs are an alternative to study genetic and pathogenic processes without the need of primary cells.

The technology of reprogramming adult, somatic cells into an embryonic stem cell-like state, resulting in so called iPSCs is a rather young technology, opening various possibilities for *in vitro* studies. In contrast to primary cell isolation, iPSCs can be generated from almost every cell type of the human body and does not require surgery in order to isolate cells, as a small skin biopsy is sufficient (Chen et al., 2016). Further, iPSCs are an almost unlimited source of target cells due to an unlimited replicative capacity (Chen et al., 2016). Patient-specific or disease-specific iPSCs of different donors reflect a more realistic population with a varying genetic background (Chen et al., 2016; MacArthur et al., 2012). *In vitro* iPSCs can be differentiated into virtually any cell type of the human body (Wobus and Boheler, 2005). Pluripotent stem cells typically express transcription factors such as Octamer-binding transcription factor 4 (*OCT4*), Nanog homeobox (*NANOG*), and sex determining region Y-box 2 (*SOX2*). The high differentiation capability of iPSCs enables investigations of vascular cell types *in vitro*. Therefore, the iPSC technology displays a good tool for identifying the function of VSMCs/vascular endothelial cells play in the development of cardiovascular diseases. Until today, only a few methods are published showing possibilities to differentiate VSMCs out of iPSCs. Older protocols, as published by Xie and colleagues in 2008, use simple but undefined methods, like adding retinoic acid to the pluripotent stem cells (PSCs) (Xie et al., 2008). Within the last years, more complex protocols for the generation of human iPSC-derived VSMCs have been published, that allow lineage specific differentiation (Cheung et al., 2014). Nevertheless, no protocol for the differentiation of human iPSC-derived calcifying vascular cells has been published until today.

2. Results

2.1. Differentiation of iPSCs into VSMCs

The following protocol was established using HFF iPSCs as a healthy control iPSC line (Zanon et al., 2017). We initially used the protocol published by Cheung and colleagues in 2014 to generate lateral mesoderm-originated VSMCs out of human pluripotent stem cells. This protocol proved less efficient to produce higher numbers of VSMCs than reported. Therefore, slight changes and new adaptations were introduced into the original protocol. Human iPSCs were grown until 80% confluency in T175 flasks. One day prior to induction of differentiation (d-1) the medium was changed from mTeSR1 to CDM-BSA supplemented with 12 ng/ml FGF2 and 10 ng/ml Activin A. For induction (d0) of differentiation into VSMCs cells were replated in a ratio of 1:3 on gelatin-coated, MEF-conditioned T75 flasks in CDM-PVA supplemented with 20 ng/ml FGF2, 10 μ M LY294002 and 10 ng/ml BMP4. Following, the complete medium was exchanged on d1.5 and d3 supplemented with 20 ng/ml FGF2 and 50 ng/ml BMP4, as suggested by Cheung and co-workers. After specification of lateral mesoderm (d5) cells were replated at a density of 25,000 cells/cm². Cells were kept in CDM-BSA medium for only 1d (d-1) until replated at a ratio of 1:3 from T175 to T75 flasks to ensure high confluency at the start of differentiation (d0). In contrast to the original protocol, cells were replated at a density of 25,000 cells/cm² on d5 in our hands, resulting in a much higher overall cell number, as well as a better dead to viable ratio (Fig. 1). This seeding density for replating on d5 was determined in a seeding assay, checking for different cell densities in a running differentiation. The use

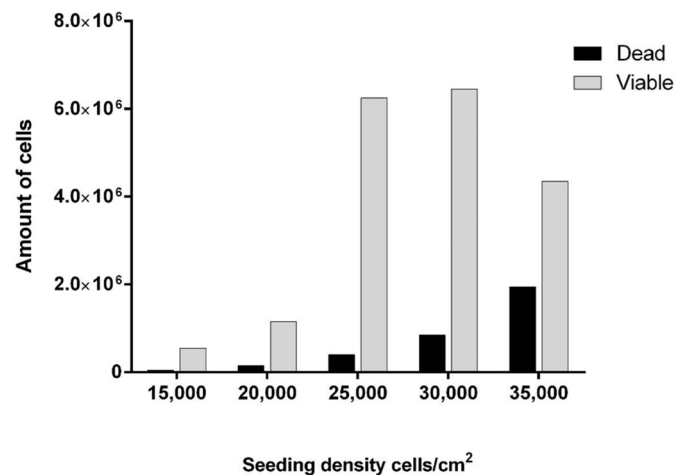


Fig. 1. Seeding density assay: On d5 of differentiation HFF cells were reseeded in different densities between 15,000 and 35,000 cells/cm² to determine the optimum cell density for a high amount of living cells at the end of the differentiation with a small amount of dead cells. $n = 1$.

of Nunc® well plates proved non-efficient, as cells died after replating on day 5 (d5). Therefore, the whole differentiation procedure was carried out on T75/T175 tissue culture flasks from Sarstedt. Starting from d5 until d18, Cheung and colleagues recommended to perform only changes of 50% of the medium every other day (Cheung et al., 2014). We instead found out that a complete medium exchange every second day, in order to wash out all dead cells, notably improved cell viability. For specification of lateral-mesoderm derived VSMCs medium was supplemented with 10 ng/ml PDGF-BB and 2 ng/ml TGF β 1. After 18 days, generated iPSC-derived VSMCs were cryopreserved in liquid nitrogen or further cultured in SMC-medium for calcification assays and other analyses. During differentiation we did not experience the necessity to passage the cells.

In addition to the HFF cell line, the iPSC line 18i-3-6 was used and differentiated as described above. Both iPSC lines were checked for correct morphology and expression of pluripotency markers such as NANOG in immunofluorescence stainings (Fig. 2). Both cells lines displayed typical iPSC morphologies and expressed NANOG in the nucleus. No differences in the expression between the iPSC lines were noticed.

2.2. Differentiation of iPSC-derived VSMCs into calcifying cells

For the generation of calcifying vascular cells, VSMCs were plated on gelatin-coated Nunc® 24-well plates for calcification at a density of 52,000 cells/cm² in SMC-medium for at least 24 h. Calcification was initiated by adding osteogenic medium to the cells and change complete medium twice a week (Fig. 3). Calcification was terminated after additional 30 days of treatment with osteogenic medium. Control cells were kept in SMC-medium during the course of calcification. All in all, the differentiation of iPSCs into calcifying VSMCs takes 49 days.

2.3. Characterization of iPSC-derived VSMCs

The differentiated cells at crucial stages of the protocol were characterized in order to ensure the right cell type in each step. Characterization was performed *via* immunofluorescence staining for CNN1 and TAGLN (Fig. 4), qPCR analyses for cell type specific gene expression markers (Fig. 6A), as well as Western Blot (WB) analyses (Fig. 6B) for cell type-corresponding protein expression. In order to ensure differentiated cells are maintaining VSMC character immunofluorescence stainings for CNN1 and TAGLN were performed (Fig. 4) showing that all VSMC-lines express both SMC-specific proteins. In order to estimate the differentiation efficiency, immunofluorescence

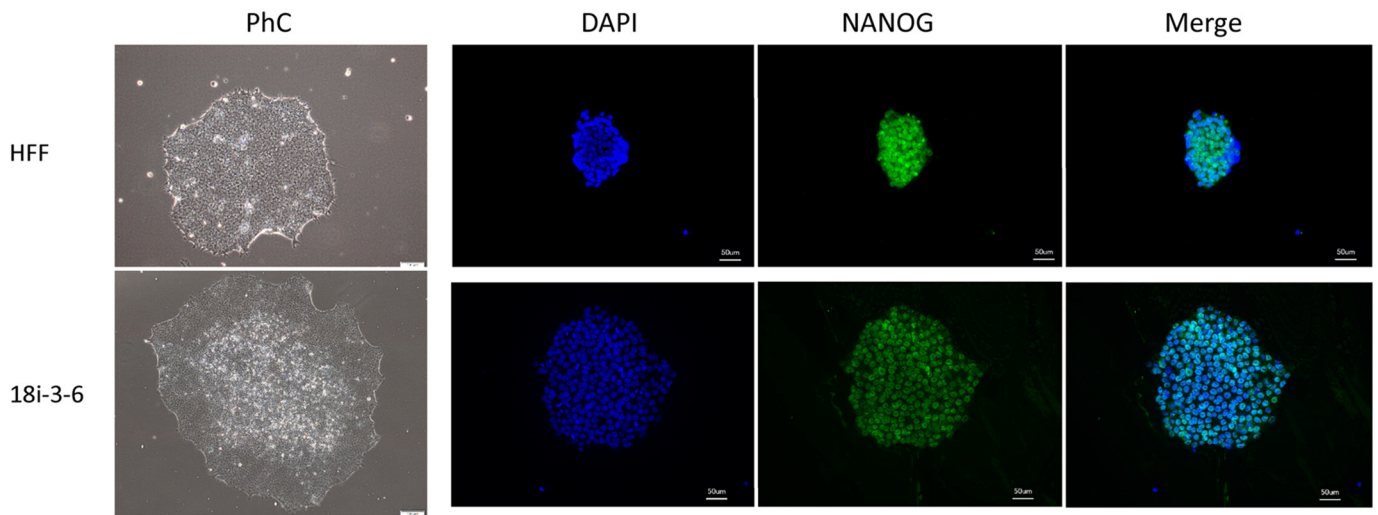


Fig. 2. Characterization of two independent iPSC-lines on cellular level: Both iPSC lines show normal colony growth as shown in brightfield images (PhC). Scale bars 100 µm; Immunofluorescence staining show DAPI (blue) localization in the nuclei, and specific nucleolar localization of the pluripotency-associated protein NANOG (green). The overlay (Merge) confirms the localization in the nuclei. Scale bars 50 µm. *n* = 2. (For interpretation of the references to colour in this figure legend, the reader is referred to the web version of this article.)

stainings of iPSC-VSMCs stained against CNN1 and TAGLN were analyzed for the expression of TAGLN and CNN1 in relation to DAPI. The analysis showed that almost all cells that express TAGLN also express CNN1. The differentiation efficiency therefore is above 90% for both cell lines (Fig. 5). No significant differences could be seen between the tested cell lines. RNA analyses of pluripotency-associated markers *NANOG*, *OCT4*, and *SOX2* showed significant downregulation of gene expression in iPSC-derived VSMCs as well as in calcifying cells (Fig. 6A). SMC marker genes *CALD1*, *CNN1*, and *TAGLN* on the other hand displayed a significant upregulation in iPSC-derived VSMCs and calcifying cells up to 10-fold compared with iPSCs (Fig. 6A). Similarly, on protein level (Fig. 6B) no *OCT4* expression was detected in VSMCs. The SMC marker *TAGLN* was found to be highly expressed in iPSC-derived VSMCs (3.5-times higher expression in iPSC-derived VSMCs than in iPSCs).

The same tendency was seen for the additional iPSC line tested with this differentiation protocol. The 18i-3-6 line also showed a significant downregulation of pluripotency-associated markers *NANOG*, *OCT4*, and

SOX2 in iPSC-derived VSMCs, whilst SMC-associated markers *CALD1*, *CNN1*, and *TAGLN* were significantly upregulated (Fig. 7A). The protein expression of *OCT4* was significantly downregulated in iPSC-derived VSMCs of the 18i-3-6 iPSC line. *TAGLN* protein expression was upregulated in iPSC-derived VSMCs (Fig. 7B).

2.4. Characterization of iPSC-derived calcifying VSMCs

After proving that the differentiation was successful, we further investigated the calcification of iPSC-derived VSMCs, analyzing their amount of CaP deposits using standard techniques such as Calcein and Alizarin Red S staining (Fig. 8A). Clearly, cells treated with osteogenic medium show high amounts of CaP deposits, represented by bright Calcein staining, whereas control cells kept in SMC-medium show no Calcein staining signal (Fig. 8A). Alizarin Red S staining shows bright red colour in calcified, osteogenic medium-treated cells, while VSMCs kept in SMC-medium appear in fade red to yellow (Fig. 8A). Calcifying events were mainly detected in the ECM, as calcifying cells excrete

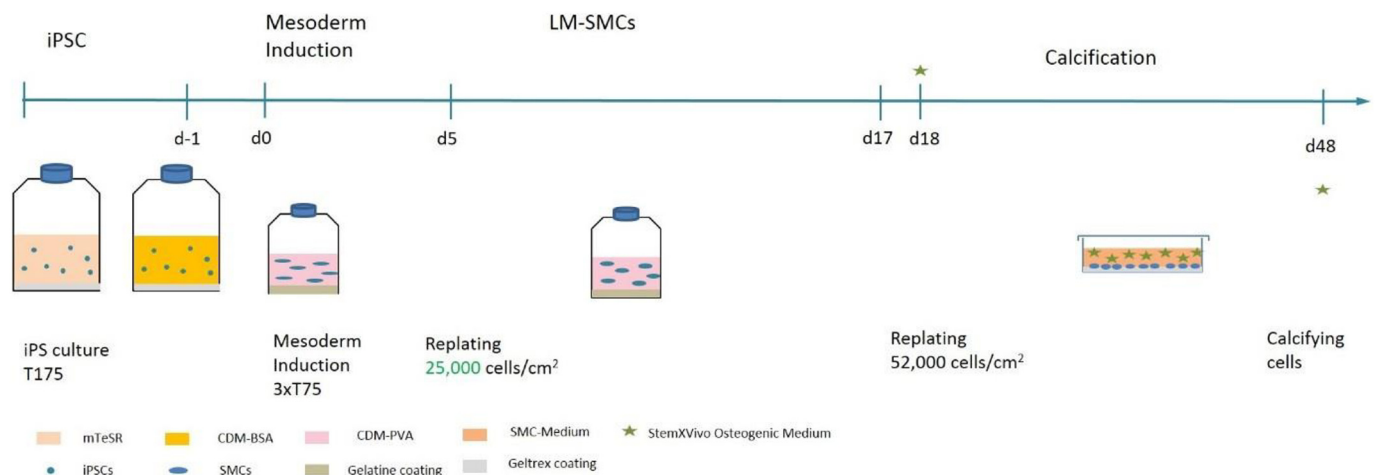


Fig. 3. Schematic view of differentiation and calcification protocol (adapted from Cheung et al., 2014): iPSCs were cultured until they were 80% confluent in T175 flasks and, subsequently, switched to CDM-BSA for 24 h (d-1). At the start of differentiation (d0) cells were replated at a ratio of 1:3 in T75 flasks in CDM-PVA medium including inducers according to the original protocol. On d5, cells were replated at a density of 25,000 cells/cm². Complete medium was exchanged every second day until d18. For calcification, cells were seeded at a density of 52,000 cells/cm² on gelatin-coated 24-well plates. Treated cells were kept in osteogenic medium for 30d, while untreated controls were kept in SMC-medium. *n* = 3.

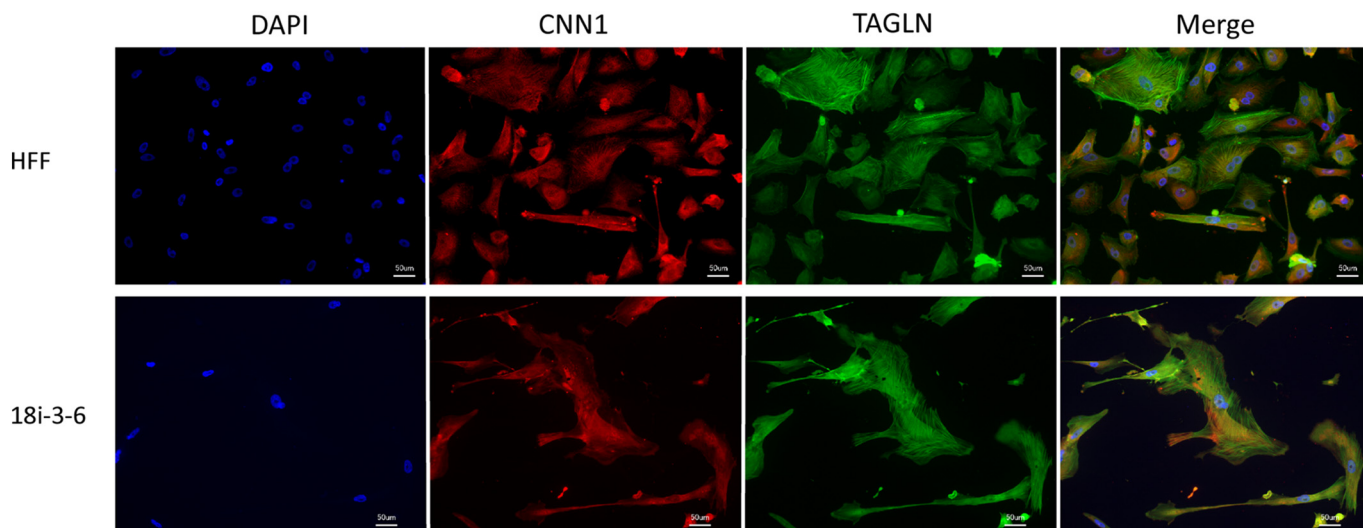


Fig. 4. Characterization of two independent iPSC-derived VSMC lines in immunofluorescence staining: All iPSC-VSMCs show the expression of VSMC marker proteins TAGLN (green) and CNN1 (red) in the cytoplasmic compartment of the cells. Nuclei are stained with DAPI (blue). The overlay (Merge) shows the colocalization of CNN1 and TAGLN in all cells. Scale bars 50 μ m. $n = 2$. (For interpretation of the references to colour in this figure legend, the reader is referred to the web version of this article.)

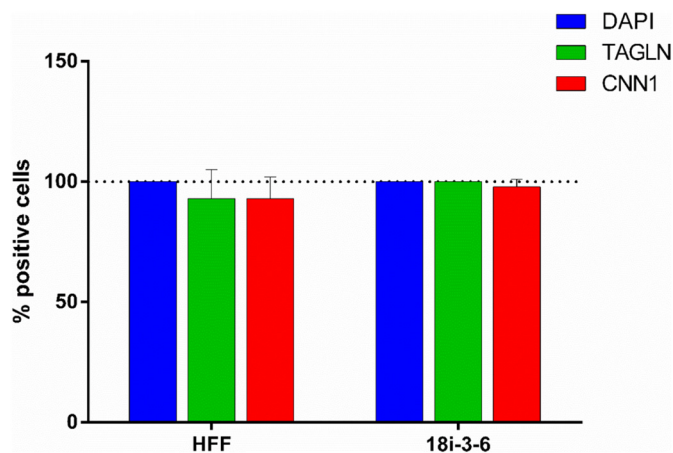


Fig. 5. Estimated differentiation efficiency in two iPSC-VSMC lines. Immunofluorescence images of the iPSC-derived VSMCs stained against CNN1 and TAGLN were analyzed regarding their percentage of fluorescent cells. Both iPSC-derived VSMCs lines show between 90 and 100% TAGLN (green) and CNN1 (red) positive cells. $n = 5$ per line. (For interpretation of the references to colour in this figure legend, the reader is referred to the web version of this article.)

more matrix and precipitate CaP into the ECM. Additionally, the degree of calcification was quantified using a Randox Calcium quantification kit. Differences between treated and untreated cells observed in the Calcein and Alizarin Red S staining were confirmed by this quantification, showing increased CaP levels in treated cells up to 5.5 times higher than in control cells (Fig. 8B).

In order to confirm the molecular regulation of the cellular calcification, qPCR for RNA and WB analyses for protein expression of the calcification markers ALP and CTSK was performed (Fig. 9). Both, qPCR and WB show the upregulation of calcification markers in calcified cells compared to untreated controls (SMC).

ALP expression is significantly upregulated on RNA level up to six-fold, while CTSK expression shows expression fold change up to 10-fold higher in calcifying, osteogenic medium-treated cells compared to the untreated control, iPSC-derived VSMCs (Fig. 9A). Additionally, upregulated expression of the calcification markers ALP and CTSK was also confirmed in WB analyses (Fig. 9B).

Conclusively, we were able to establish a protocol for the differentiation of human iPSCs towards lateral plate mesoderm-derived VSMCs. The successful differentiation, using an adapted protocol formerly published by Cheung and colleagues, was confirmed by IF staining for SMC markers CNN1 and TAGLN, as well as qPCR and WB analyses showing significant downregulation of the iPSC markers SOX2, NANOG, and OCT4, and a simultaneous upregulation of SMC markers CALD1, CNN1, and TAGLN. Additionally, the morphology of the cells was appropriate to the expected cell type. The subsequent calcification of iPSC-derived VSMCs using osteogenic medium was also successful as confirmed by Calcein and Alizarin Red S staining, as well as a Calcium assay for the quantification of CaP deposits. Both, staining and quantification, showed high levels of CaP in osteogenic medium-treated cells and very low to no CaP deposits in untreated controls. Similarly, molecular analyses on mRNA and protein level showed upregulation of calcification-specific markers ALP and CTSK, validating the findings from the staining. These results show that human iPSC-derived VSMCs were successfully transformed into calcifying vascular cells after induction with osteogenic medium.

3. Discussion

Vascular calcification is known as the deposition of CaP mineral in cardiovascular tissues like arteries and heart valves (Jono et al., 2000a). Pathological calcification goes hand in hand with the formation of atherosclerotic lesions (Aherrahrou and Schunkert, 2013). As a consequence, vascular calcification leads to a three- to four-fold increase in the risk of cardiovascular morbidity and mortality (Alam et al., 2009). Various risk variants have been identified within the last years to be associated with calcification through GWA studies, making it necessary to go beyond GWAS and find relevant *in vitro* assays to first functionally link the risk variants with calcification or atherosclerosis. This may help thereafter, at long term, to identify novel pathways that can be targeted by drugs. Very recently we reported successful drug treatment for the cardiac calcification causing gene Abcc6 with Etidronate (Pomozzi et al., 2017; Bauer et al., submitted). As primary vascular cells are hardly accessible and quickly lose their typical properties, thus less dynamic, these cells are less suitable for *in vitro* studies (Alexander and Owens, 2012). The iPSC-technology enables such studies *in vitro* without putting patients at risk for the extraction of cells. Differentiation protocols of iPSCs towards vascular cells have been published before (Cheung

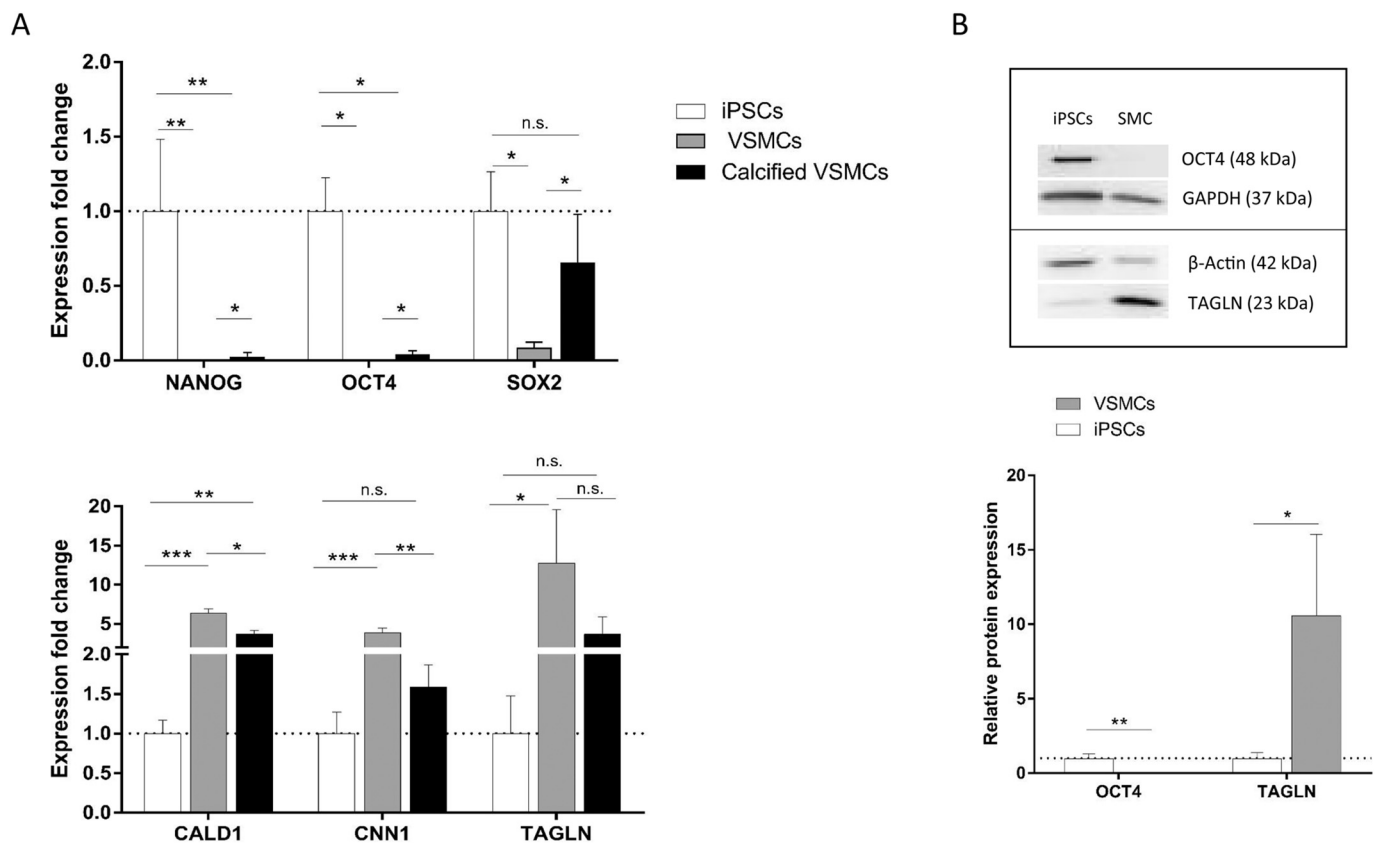


Fig. 6. Molecular analyses of HFF iPSCs, iPSC-VSMCs and calcified cells: A) RNA expression analyses show downregulation of the pluripotency markers *NANOG*, *OCT4*, and *SOX2* in treated and untreated iPSC-derived VSMCs compared to iPSCs. The SMC-marker genes *CALD1*, *CNN1*, and *TAGLN* were upregulated in both, treated and untreated iPSC-derived VSMCs compared to iPSCs. All expression levels were normalized to β -Actin and iPSCs. Data are presented as mean + SD. $n = 9$; B) Protein expression analyses confirm downregulation of the pluripotency marker *OCT4* in iPSC-derived VSMCs and upregulation of the SMC-marker *TAGLN* in iPSC-derived VSMCs. Representative Blots are displayed above. *OCT4* was normalized to *GAPDH*, *TAGLN* was normalized to β -Actin. Quantification of WB is shown below. Data are presented as mean + SD. $n = 3$ (*OCT4*); $n = 4$ (*TAGLN*).

et al., 2014; Xie et al., 2008), but there are no protocols for the calcification of human iPSC-derived VSMCs *in vitro* until today.

The differentiation protocol for iPSCs into lateral mesoderm-derived VSMCs was adapted from Cheung et al., 2014. In order to adapt the protocol for our cell line, various changes were performed, including higher cell seeding densities and complete medium exchange instead of 50%. iPSCs and differentiated cells were checked on RNA and protein level regarding cell type specific marker expression, proving the correct properties of the respective cell type. Overall, we were successful in adapting the protocol originally published by Cheung et al., 2014 for our cell line. Nonetheless, various changes were introduced in order to accomplish high differentiation efficiencies. In fact, it has been reported previously, that iPSC lines of different donors or even clones of the same line display a high variability regarding their differentiation susceptibility and efficiency (Hu et al., 2010; Ramos-Mejia et al., 2010). Therefore, it is likely that the necessity to adapt the original differentiation protocol to our cell line is caused by this PSC variability. After applying this differentiation method to another iPSC donor line we observed similar reactions to the differentiation protocol, implying it works for other donor cell lines as well.

To enhance calcification in iPSC-derived VSMCs, the differentiation protocol was extended with an additional calcification period, during which cells were treated with osteogenic medium for further 30d. As published previously, various methods exist today to calcify or mineralize primary human, murine or bovine VSMCs such as supplementation with β -glycerophosphate, L- ascorbic acid or inorganic phosphate (Pi, ≥ 2 mM) (Byon et al., 2008; Tintut et al., 2003; Wada et al., 1999; Yang et al., 2004). All methods showed calcification *in vitro* in a

concentration- as well as time-dependent manner. For our study, we initially used Pi and β -glycerophosphate based media. Pi turned out to be inappropriate for our experiments, as massive cell death and detaching of cells appeared during the first days of calcification. Therefore, we decided to use StemXVivo[®] human osteogenic medium that uses β -glycerophosphate as calcification agent and is serum-free. Papers dealing with *in vitro* calcification reported clear increase of calcium depositions shown by quantifications. Additionally, stainings like von Kossa or Alizarin Red S were used to demonstrate increased calcification (Jono et al., 2000b; Reynolds et al., 2004; Wada et al., 1999). In order to verify successful calcifications in our experiments we used similar standard methods, including Alizarin Red S and Calcein staining, calcium quantification and osteogenic marker gene expression analyses. In the end, we were able to show concurrent results as obtained with primary human, bovine or murine cells, such as increased calcium depositions in staining, as well as upregulation of calcification-associated gene and protein expressions.

Finally, the differentiation of the HFF iPSC line (Zanon et al., 2017) into lateral-plate mesoderm-derived VSMCs as well as calcifying vascular cells is a stable working process, enabling the *in vitro* study of atherosclerosis with easily-accessible, phenotypically more consistent VSMCs. For future studies, somatic cells, such as skin cells, from patients carrying CAD risk variants, as well as healthy controls, will be isolated and reprogrammed into iPSCs (Fig. 10). Afterwards, iPSCs will be differentiated into calcifying VSMCs following the protocol we have presented here. Cells from risk patients will then be compared with healthy controls. In this way, we will be able to clarify how the risk variants contribute to the development of CAD and calcification in

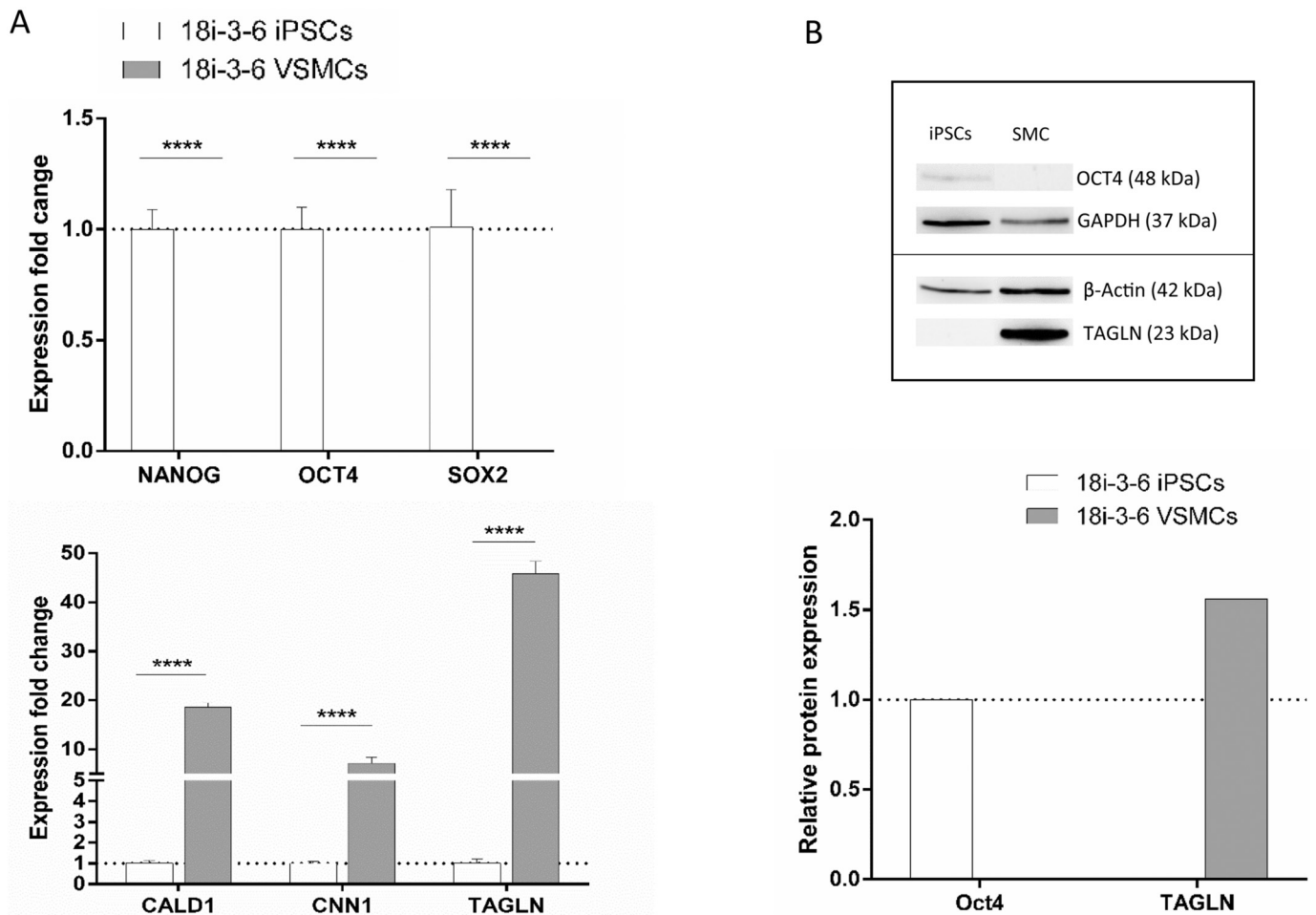


Fig. 7. Molecular characterization of 18i-3-6 iPSC-derived VSMCs. RNA expression of *NANOG*, *OCT4*, and *SOX2* show significant downregulation in iPSC-derived VSMCs compared to iPSCs. RNA expression of SMC markers *CALD1*, *CNN1*, and *TAGLN* is upregulated in iPSCs. $n = 1$. Protein expression analyses show the downregulation of *OCT4* in VSMCs and upregulation of *TAGLN* expression for VSMCs. $n = 1$.

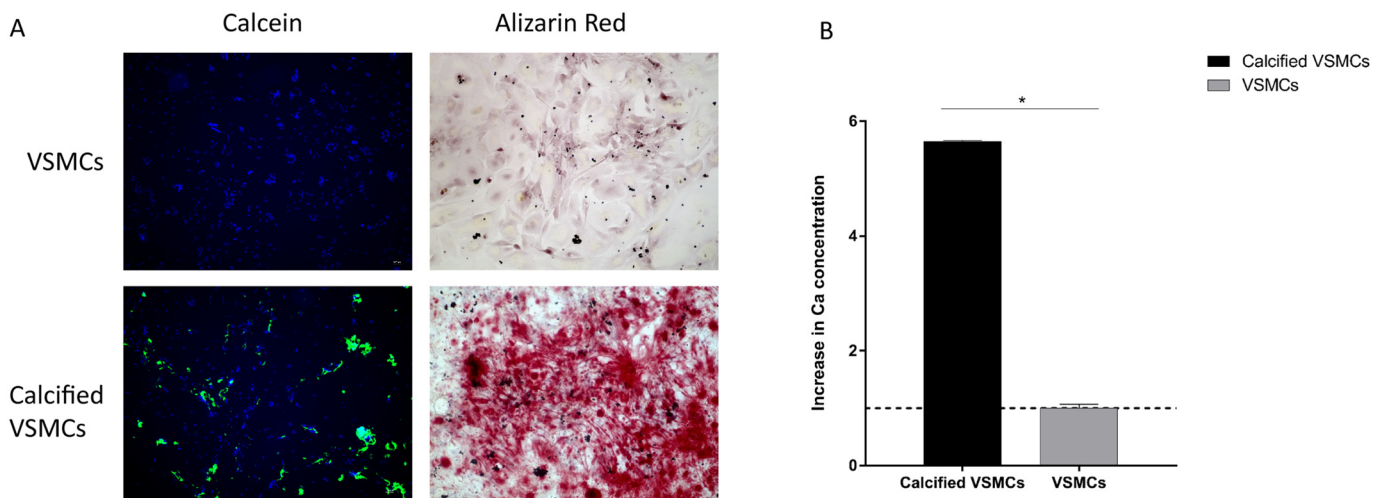


Fig. 8. Colorimetric localization and quantification of cellular calcification: A) Calcification was shown via Calcein staining (left), where nuclei are counterstained with DAPI (blue) and calcium deposits are stained with calcein (green). Alizarin Red S staining (right) displays calcium deposits in red, while non-calcified cells appear pale. Control cells were maintained in SMC-medium (VSMC), treated cells were kept in osteogenic medium (Calcified VSMCs) for 30 d. $n = 4$. B) Calcification was quantified with the help of a colorimetric Calcium assay. Control cells were maintained in SMC-medium (VSMC), treated cells were kept in osteogenic medium (Calcified VSMCs) for 30d. Calcification levels were normalized to untreated controls ($n = 4$). Data are presented as mean + SD. (For interpretation of the references to colour in this figure legend, the reader is referred to the web version of this article.)

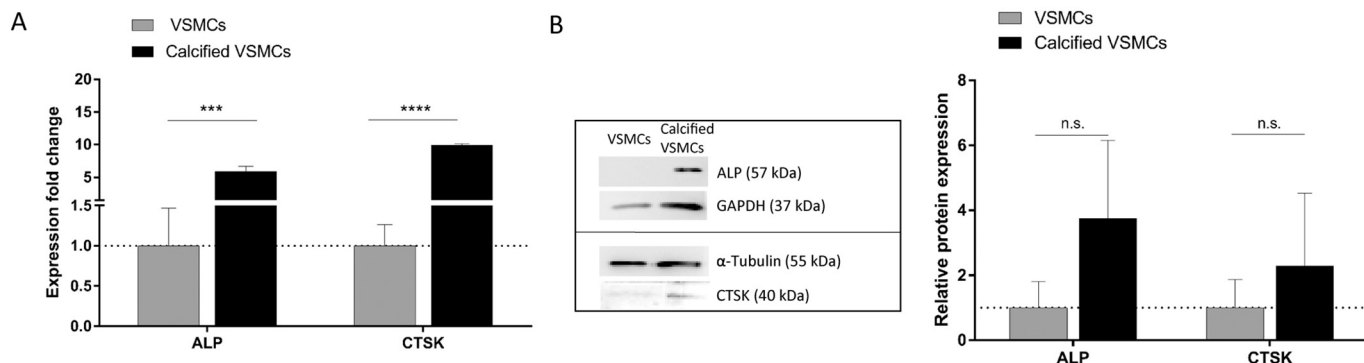


Fig. 9. Molecular analysis of cellular calcification: A) VSMCs treated with osteogenic medium (Calcified VSMCs) show significantly increased expression of calcification markers *ALP* and *CTSK* on mRNA level. Expression levels were normalized to β -Actin and untreated cells (VSMCs). Data are presented as mean + SD. $n = 9$. B) Cells treated with osteogenic medium show increased protein expression of calcification markers *ALP* and *CTSK* in WB analysis. Representative WB images are shown on the left, quantification of WB is shown on the right. Data are presented as mean + SD. $n = 3$.

particular.

Furthermore, thanks to the CRISPR/Cas9 technology it is easily achievable to create knockout (KO) cell lines for various atherosclerosis- or calcification-associated genes or loci, like 9p21, *PHACTR1*, *ADAMTS7*, *MRAS*, and *COL4a1/a2* (Webb et al., 2017) to determine their functional link to vascular calcification and better understand the respective underlying mechanisms. Moreover, gene editing may be applied using CRISPR/Cas, giving the opportunity to specifically examine the GWAS risk variants identified in patients in regard to atherosclerosis and CAD.

4. Experimental procedures

4.1. Cell culture, VSMC differentiation and calcification

Human foreskin fibroblasts were isolated as described previously (Zanon et al., 2017). Briefly, for reprogramming of the fibroblasts they were transfected with pMIG vectors containing the pluripotency factors OCT4, SOX2, c-MYC, and KLF4 (Zanon et al., 2017). The human iPSC line, iPS-HFF-wt (Zanon et al., 2017), was kindly provided by the Institute of Neurogenetics, University of Luebeck, and was adapted to Geltrex® (Thermo Fisher, #A1569601) coating and maintained in mTeSR™1 (Stemcell Technologies, #05850) medium. Cells were passaged enzymatically with StemPro® Accutase® Cell Dissociation Reagent (Thermo Fisher Scientific, #A1110501) once a week at a ratio of

1:6 to 1:10. Further, the iPSC line USCD018i-3-6 (referred to as 18i-3-6; WiCell) was used to prove the differentiation protocols' successful application to other iPSC lines. The 18i-3-6 are reprogrammed from skin fibroblasts with the use of Sendai virus. The 18i-3-6 iPSC line was maintained as described above.

For VSMC differentiation, the protocol published by Cheung and co-workers was adapted and changed slightly, in order to increase efficiency (Cheung et al., 2014). For details please see the Results section. The differentiation media were composed as published previously (Cheung et al., 2014). Differentiated VSMCs were cultivated in SMC-medium composed of Dulbecco's Modified Eagle Medium with high glucose and GlutaMAX (Thermo Fisher Scientific, #10566016), supplemented with 10% fetal bovine serum (FBS; Pan Biotech) and 1% Penicillin/Streptomycin.

For calcification, iPSC-derived VSMCs were replated at a density of 52,000 cells/cm² in Nunc® 24-well cell culture plates and cultured in StemXVivo® human osteogenic medium (R&D Systems, #CCM008/CCM007; referred to as osteogenic medium) for another 30 days. All experiments were carried out in 3 biological replicates and at least 3 technical replicates in independent experiments, unless stated otherwise.

4.2. Calcium assay

In order to determine the CaP concentration, the cells were washed

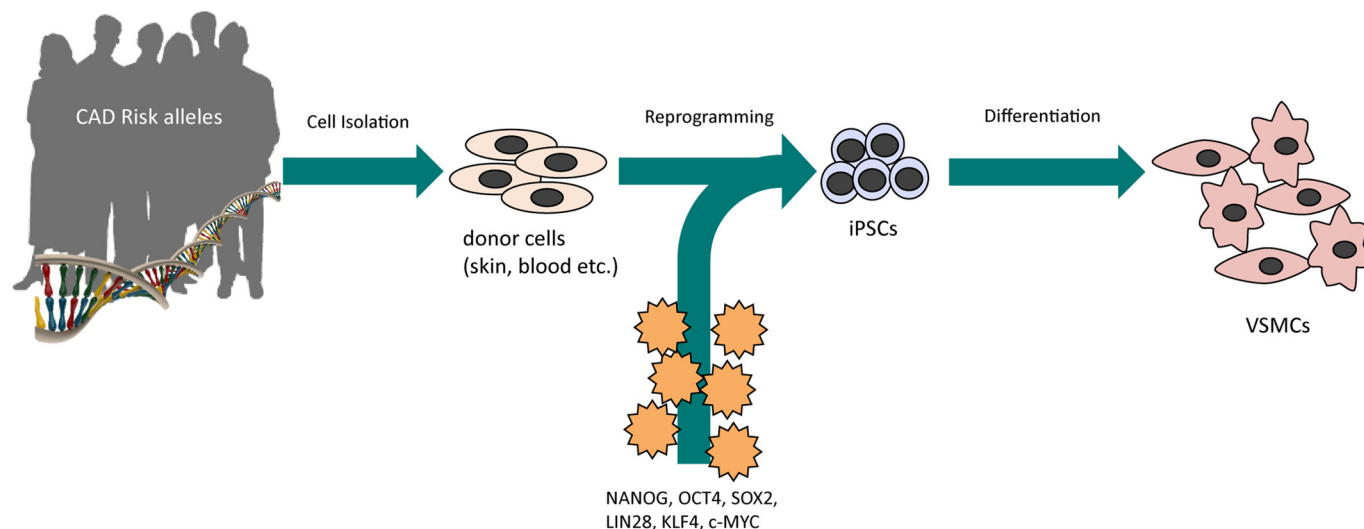


Fig. 10. Study design: Cells from patients with CAD risk variants as well as healthy controls are isolated and reprogrammed into iPSCs. Afterwards, iPSCs are differentiated into VSMCs and calcifying vascular cells.

twice with PBS and incubated with 0.6 N HCl overnight at 4 °C. On the next day, CaP content in the supernatant was determined following the protocol of the Randox Calcium quantification assay (Randox, #CA590).

4.3. Calcein staining

For Calcein staining, cells were fixed in cold 4% PFA for 30 min. PFA was discarded and cells were incubated with Calcein working solution (1:1000, TBS, pH 9) for 30 mins in the dark. Following the incubation, cells were washed three times in TBS (pH 9) for 3 mins each. Nuclei were stained with 4',6-diamidino-2-phenylindole (DAPI) solution for 10 mins in the dark. Finally, cells were again washed with TBS for 3 mins and subsequently coated with TBS for imaging. Fluorescent images were taken, using a Keyence BZ-9000 microscope.

4.4. Alizarin Red S staining

Cells were fixed in cold 4% PFA for 30 min and subsequently washed with distilled water. Osteogenesis of iPSC-derived calcifying VSMCs was determined using Alizarin Red S staining (Osteogenesis Assay Kit, Millipore, #ECM815) following the manufacturers' instructions. Representative images were taken using a Keyence BZ-9000 microscope.

4.5. RNA isolation and quantitative PCR (qPCR)

RNA isolation of cells was performed using the Qiagen RNeasy Mini Plus Kit (Qiagen, #74136) following manufacturers' instructions. Synthesis of cDNA from RNA templates via reverse transcription was performed as follows: 10 µl of RNA sample, adjusted to a concentration of 100 ng/µl in DNase/RNase-free water (Gibco, #10977035), was incubated for 5 min at 68 °C. 10 µl of the reaction mix for reverse transcription, containing 4 µl 5× First Strand Buffer (Invitrogen, #28025021), 2 µl 100 mM dithiothreitol (DTT) (Invitrogen, #28025021), and 1 µl 4 mM dNTPs (Promega, #U1330), Random Hexamer Primer-Mix (Roth, #HP28.1), RiboLock (40 U/µl) (Thermo Scientific, #EO0381), and M-MLV RT (200 U/µl) (Invitrogen, #28025021) each, was added to the RNA and incubated for 1 h at 37 °C, followed by enzyme inactivation at 95 °C for 5 min. Quantitative gene expression analysis was performed on a 7900HT Fast Real-Time PCR System (Applied Biosystems, #4329001) using the corresponding SDS 2.2.2 software for analysis. The reaction mix consisted of 3.75 µl PowerUp™ SYBR® Green Master Mix (Life Technologies, #A25777), 1.125 µl Primer mix (5 pmol/µl) and 1.125 µl DNase/RNase-free water (Gibco, #10977035), as well as 1.5 µl of cDNA, respectively. Gene expression was normalized to the internal standard β -Actin (for primer sequences see Supplementary Material Table S1).

4.6. Protein isolation

Adherent cells were detached by incubation with StemPro Accutase® Cell Dissociation Reagent (Life Technologies, #A11105–01). The cell suspension was washed with 1× phosphate buffered saline (PBS) prior to resuspension in 100–200 µl cell lysis buffer. Complete cell lysis buffer consists of 10 µl phenylmethane sulfonyl fluoride (PMSF) (Sigma Aldrich, #P7626), 100 µl 25× Protease Inhibitor (Roche, #1169749800), 100 µl 10× cell lysis buffer (Cell Signaling, #9803) and 750 µl DNase/RNase-free water (Gibco, #10977035), supplemented with 16.7 µl DNase I (RNase-Free DNase Set, Qiagen, #79254).

4.7. Western Blot (WB)

The polyacrylamide gels were prepared in glass plates fixed in a casting module (BioRad, Hercules, USA) with a resolving gel of 10 to 12% and 4% stacking gel. 5 µl of 3× SDS Loading Buffer (BioLabs,

#B7703S), supplemented with 1.25 M DTT (BioLabs, #B7703S) at a ratio of 10:1, was added to 10 µl of each sample, containing 10 µg of total protein. Samples were heated at 95 °C for 5 min and placed on ice until use. Precision Plus Protein Dual Colour Standard (BioRad, #161–0374) served as a size standard. The proteins were separated for about 2 h at 100 V. For transfer to a PVDF Immobilon-P Membrane (Millipore, #IPVH00010), proteins were blotted for 1 h at 120 V. The detection of specific proteins was performed by antibody staining. Unspecific binding sites on the membrane were blocked with 5% milk solution at 4 °C for 1 h. Subsequently, the membrane was incubated with a primary antibody binding to the target protein (for list of antibodies see Supplementary Material Table S2) at 4 °C overnight. The membrane was incubated for 1 h with a horseradish peroxidase (HRP)-coupled secondary antibody in 5% milk (for list of antibodies see Supplementary Table S2) according to the host of the primary antibody. For visualization of the antibody staining, ECL Prime Western Blotting Detection Reagent (GE Healthcare, #RPN2232) was directly added to the membrane and the chemiluminescence was detected using a Chemi Doc XRS BioRad imaging system (BioRad, Hercules, USA). Protein expression was quantified using the Image Lab Software (BioRad, Hercules, USA). GAPDH, α -Tubulin or β -Actin served as internal standard for target protein quantification.

4.8. Immunofluorescence staining (IF)

For IF analysis cells were grown on Nunc™ Lab-Tek™ II Chamber Slides™ (Thermo Scientific, #154534) at a seeding density of 0.5×10^4 to 2×10^4 cells per cm². Cells were washed with PBS and then fixed 30 min with chilled (–20 °C) methanol:acetone solution (1:1). For antibody staining, cells were permeabilized in PBS containing 0.1% Triton-X 100 (Sigma Aldrich, #T-8787) and 1% bovine serum albumin (BSA) and blocked with PBS containing 3.5% BSA. 100 µl primary antibody diluted in blocking solution (for list of antibodies see Supplementary Material Table S3) or blocking solution alone in case of the negative control, was applied to each well and incubated overnight at 4 °C. Slides were incubated with a secondary antibody (1:500) diluted in PBS for 1 h at room temperature. To counterstain the nucleus of the cells they were incubated with DAPI solution for 10 mins in the dark. The slides were covered using Dako Fluorescence mounting medium (Dako, #S3023) and cover slips (Menzel, #9161060). The detection of IF staining was performed with a Keyence BZ-9000 fluorescence microscope (Keyence, Neu-Isenburg, Germany).

4.9. Analysis of differentiation efficiency using IF images

IF images of iPSC-derived VSMCs stained against CNN1 and TAGLN were used for the analysis of differentiation efficiency. DAPI stained nuclei were counted and used as total number of cells. TAGLN and CNN1 positive cells in the single fluorescent channels were counted. Finally, the percentage of CNN1 and TAGLN positive cells compared to DAPI were estimated, resulting in the differentiation efficiency.

4.10. Statistical analyses

Data are presented as means + SD. Unpaired *t*-tests were performed using GraphPad. *P* < .05 was considered statistically significant. For all tests: **P* < .05, ***P* < .01, ****P* < .001, *****P* < .0001 and n.s. for not significant.

Author contributions

A.T. carried out and analyzed the majority of experiments, was involved in the project design and wrote the majority of the manuscript. U.H. and A.R. were involved in the establishment of the differentiation and calcification protocols. M.M. and B.S. were involved in the maintenance of iPSCs and establishment of the differentiation protocol. M.T.

and P.S. provided resources and expertise in iPSC technology. R.A. assisted with the calcification protocol. J.E. and Z.A. contributed to the project design, editing and writing of the manuscript, as well as collecting funding.

Acknowledgements

We thank Sandra Wrobel, Sabine Stark, Annett Liebers and Maren Behrensen for their excellent technical assistance.

Sources of funding

This study was funded by a grant from the Fondation Leducq (12CVD02; CADgenomics: Understanding Coronary Artery Disease Genes). P.S. is supported by the German Research Foundation (FOR2488).

Appendix A. Supplementary data

Supplementary data to this article can be found online at <https://doi.org/10.1016/j.scr.2018.07.008>.

References

- Aherrahrou, Z., Schunkert, H., 2013. Genetics of atherosclerosis and vascular calcification go hand-in-hand. *Atherosclerosis* 228, 325–326.
- Aherrahrou, R., Aherrahrou, Z., Schunkert, H., Erdmann, J., 2017. Coronary artery disease associated gene Phactr1 modulates severity of vascular calcification in vitro. *Biochem. Biophys. Res. Commun.* 491, 396–402.
- Alam, M., Kirton, J.P., Wilkinson, F.L., Towers, E., Sinha, S., Rouhi, M., Vizard, T.N., Sage, A.P., Martin, D., Ward, D.T., et al., 2009. Calcification is associated with loss of functional calcium-sensing receptor in vascular smooth muscle cells. *Cardiovasc. Res.* 81, 260–268.
- Alexander, M.R., Owens, G.K., 2012. Epigenetic control of smooth muscle cell differentiation and phenotypic switching in vascular development and disease. *Annu. Rev. Physiol.* 74, 13–40.
- Balderman, J.A.F., Lee, H.-Y., Mahoney, C.E., Handy, D.E., White, K., Annis, S., Lebeche, D., Hajjar, R.J., Loscalzo, J., Leopold, J.A., 2012. Bone morphogenetic protein-2 decreases microRNA-30b and microRNA-30c to promote vascular smooth muscle cell calcification. *J. Am. Heart Assoc.* 1, e003905.
- Byon, C.H., Javed, A., Dai, Q., Kappes, J.C., Clemens, T.L., Darley-Usmar, V.M., McDonald, J.M., Chen, Y., 2008. Oxidative stress induces vascular calcification through modulation of the osteogenic transcription factor Runx2 by AKT signaling. *J. Biol. Chem.* 283, 15319–15327.
- Chen, I.Y., Matsa, E., Wu, J.C., 2016. Induced pluripotent stem cells: at the heart of cardiovascular precision medicine. *Nat. Rev. Cardiol.* 13, 333–349.
- Cheung, C., Bernardo, A.S., Pedersen, R.A., Sinha, S., 2014. Directed differentiation of embryonic origin-specific vascular smooth muscle subtypes from human pluripotent stem cells. *Nat. Protoc.* 9, 929–938.
- Dash, B.C., Jiang, Z., Suh, C., Qyang, Y., 2015. Induced pluripotent stem cell-derived vascular smooth muscle cells: methods and application. *Biochem. J.* 465, 185–194.
- Doherty, T.M., Asotra, K., Fitzpatrick, L.A., Qiao, J.-H., Wilkin, D.J., Detrano, R.C., Dunstan, C.R., Shah, P.K., Rajavashisth, T.B., 2003. Calcification in atherosclerosis: bone biology and chronic inflammation at the arterial crossroads. *Proc. Natl. Acad. Sci. U. S. A.* 100, 11201–11206.
- Drake, F.H., Dodds, R.A., James, I.E., Connor, J.R., Debouck, C., Richardson, S., Lee-Rykaczewski, E., Coleman, L., Rieman, D., Barthlow, R., et al., 1996. Cathepsin K, but not Cathepsins B, L, or S, is abundantly expressed in human osteoclasts. *J. Biol. Chem.* 271, 12511–12516.
- Hu, B.-Y., Weick, J.P., Yu, J., Ma, L.-X., Zhang, X.-Q., Thomson, J.A., Zhang, S.-C., 2010. Neural differentiation of human induced pluripotent stem cells follows developmental principles but with variable potency. *Proc. Natl. Acad. Sci.* 107, 4335–4340.
- Jono, S., McKee, M.D., Murry, C.E., Shioi, A., Nishizawa, Y., Mori, K., Morii, H., Giachelli, C.M., 2000a. Phosphate regulation of vascular smooth muscle cell calcification. *Circ. Res.* 87, e10–e17.
- Jono, S., Peinado, C., Giachelli, C.M., 2000b. Phosphorylation of Osteopontin is required for inhibition of vascular smooth muscle cell calcification. *J. Biol. Chem.* 275, 20197–20203.
- Lutgens, S.P.M., Cleutjens, K.B.J.M., Daemen, M.J.A.P., Heeneman, S., 2007. Cathepsin cysteine proteases in cardiovascular disease. *FASEB J.* 21, 3029–3041.
- MacArthur, C.C., Fontes, A., Ravinder, N., Kuninger, D., Kaur, J., Bailey, M., Taliana, A., Vemuri, M.C., Lieu, P.T., 2012. Generation of Human-Induced Pluripotent Stem Cells by a Nonintegrating RNA Sendai Virus Vector in Feeder-Free or Xeno-Free Conditions.
- Pomozzi, V., Brampton, C., van de Wetering, K., Zoll, J., Calio, B., Pham, K., Owens, J.B., Marh, J., Moisyadi, S., Váradi, A., et al. (2017). Pyrophosphate supplementation prevents chronic and acute calcification in ABCC6-deficient mice. *Am. J. Pathol.* 187, 1258–1272.
- Ramos-Mejia, V., Melen, G.J., Sanchez, L., Gutierrez-Aranda, I., Ligerio, G., Cortes, J.L., Real, P.J., Bueno, C., Menendez, P., 2010. Nodal/Activin signaling predicts human pluripotent stem cell lines prone to differentiate toward the hematopoietic lineage. *Mol. Ther.* 18, 2173–2181.
- Reynolds, J.L., Joannides, A.J., Skepper, J.N., McNair, R., Schurgers, L.J., Proudfoot, D., Jahnke-Dechent, W., Weissberg, P.L., Shanahan, C.M., 2004. Human vascular smooth muscle cells undergo vesicle-mediated calcification in response to changes in extracellular calcium and phosphate concentrations: a potential mechanism for accelerated vascular calcification in ESRD. *J. Am. Soc. Nephrol.* 15, 2857–2867.
- Samani, N.J., Erdmann, J., Hall, A.S., Hengstenberg, C., Mangino, M., Mayer, B., Dixon, R.J., Meitinger, T., Braund, P., Wichmann, H.-E., et al., 2007. Genomewide association analysis of coronary artery disease. *N. Engl. J. Med.* 357, 443–453.
- Schunkert, H., König, I.R., Kathiresan, S., Reilly, M.P., Assimes, T.L., Holm, H., Preuss, M., Stewart, A.F.R., Barbalic, M., Gieger, C., et al. (2011). Large-scale association analysis identifies 13 new susceptibility loci for coronary artery disease. *Nat. Genet.* 43, 333–338.
- The CARDIoGRAMplusC4D Consortium, 2013. Large-scale association analysis identifies new risk loci for coronary artery disease. *Nat. Genet.* 45, 25–33.
- Thompson, B., Towler, D.A., 2012. Arterial calcification and bone physiology: role of the bone-vascular axis. *Nat. Rev. Endocrinol.* 8, 529–543.
- Tintut, Y., Alfonso, Z., Saini, T., Radcliff, K., Watson, K., Boström, K., Demer, L.L., 2003. Multilineage potential of cells from the Artery Wall. *Circulation* 108, 2505–2510.
- Torpy, J.M., Burke, A.E., Glass, R.M., 2009. Coronary heart disease risk factors. *JAMA* 302, 2388.
- Wada, T., McKee, M.D., Steitz, S., Giachelli, C.M., 1999. Calcification of vascular smooth muscle cell cultures inhibition by Osteopontin. *Circ. Res.* 84, 166–178.
- Webb, T.R., Erdmann, J., Stirrups, K.E., Stitzel, N.O., Masca, N.G.D., Jansen, H., Kanoni, S., Nelson, C.P., Ferrario, P.G., König, I.R., et al., 2017. Systematic evaluation of Pleiotropy identifies 6 further loci associated with coronary artery disease. *J. Am. Coll. Cardiol.* 69, 823–836.
- Wilson, P.W.F., D'Agostino, R.B., Levy, D., Belanger, A.M., Silbershatz, H., Kannel, W.B., 1998. Prediction of coronary heart disease using risk factor categories. *Circulation* 97, 1837–1847.
- Wobus, A.M., Boheler, K.R., 2005. Embryonic stem cells: prospects for developmental biology and cell therapy. *Physiol. Rev.* 85, 635–678.
- Xie, C.-Q., Huang, H., Wei, S., Song, L.-S., Zhang, J., Ritchie, R.P., Chen, L., Zhang, M., Chen, Y.E., 2008. A comparison of murine smooth muscle cells generated from embryonic versus induced pluripotent stem cells. *Stem Cells Dev.* 18, 741–748.
- Yang, H., Curinga, G., Giachelli, C.M., 2004. Elevated extracellular calcium levels induce smooth muscle cell matrix mineralization in vitro. See editorial by Towler, p. 2467. *Kidney Int.* 66, 2293–2299.
- Zanon, A., Kalvakuri, S., Rakovic, A., Foco, L., Guida, M., Schwienbacher, C., Serafin, A., Rudolph, F., Trilck, M., Grünewald, A., et al., 2017. SLP-2 interacts with Parkin in mitochondria and prevents mitochondrial dysfunction in Parkin-deficient human iPSC-derived neurons and drosophila. *Hum. Mol. Genet.* 26, 2412–2425.